

Nanoscopic Quantum Rings: A New Perspective

Tapash Chakraborty

Institute of Mathematical Sciences,
Chennai 600 113, India

Abstract. With rapid advances in fabrication of nano-scale devices, quantum rings of nanometer dimensions that are disorder free and contain only a few (interacting) electrons have gained increasing attention. Accordingly, the emphasis of theoretical research has also shifted from the problems involving the persistent current which is indirectly related to the energy levels, to a direct probe of the low-lying energy spectrum of a single quantum ring. Transport and optical spectroscopies have revealed many interesting aspects of the energy spectra that are in good agreement with the theoretical picture presented here.

1 Introduction

A metallic ring of mesoscopic dimension in an external magnetic field is known to exhibit a wide variety of interesting physical phenomena. One spectacular effect that has fascinated researchers over a few decades is that the ring can carry an equilibrium current (the so-called persistent current) [1,2] which is periodic in the Aharonov-Bohm (AB) flux Φ [3,4] with a period $\Phi_0 = hc/e$, the flux quantum. This effect is a direct consequence of the properties of the eigenfunctions of isolated rings, which cause the periodicity of all physical quantities. The reason for this behavior is well known and is briefly as follows: In a ring which encloses a magnetic flux Φ , the vector potential can be eliminated from the Schrödinger equation by introducing a gauge transformation. The result is that the boundary condition is modified as $\psi_n(x+L) = e^{2\pi i\Phi/\Phi_0}\psi_n(x)$, where L is the ring circumference¹. The situation is then analogous to the one-dimensional Bloch problem with Bloch wave vector $k_n = (2\pi/L)\Phi/\Phi_0$. The energy levels E_n and other related physical quantities are therefore periodic in Φ_0 . For a time-independent flux Φ , the equilibrium current (at $T = 0$) associated with state n is

$$I_n = -\frac{ev_n}{L} = -c\frac{\partial E_n}{\partial \Phi}, \quad (1)$$

where $v_n = \partial E_n/\hbar\partial k_n = (Lc/e)\partial E_n/\partial \Phi$ is the velocity of state n . An important condition for I_n to be nonzero is that the wave functions of the charge

¹ The magnetic flux Φ is assumed to thread the ring axially but the electron motion is uninfluenced by the magnetic field. Then the Φ_0 periodicity of the electron wave function is strictly AB type.

carriers should stay coherent along the circumference L of the ring. The ring geometry and the thermodynamic current have also played a central role in the gauge-invariance interpretation of the integer quantum Hall effect and the current carrying edge states [5]. The phenomenon is restricted only to *mesoscopic* rings, i.e., rings whose size is so small that the orbital motion of electrons in the ring remains quantum phase coherent throughout.

Strictly one-dimensional rings – Büttiker et al. [2] were the first to propose the possibility of observing a persistent current in diffusive normal metal rings. They considered a one-dimensional ring enclosing a magnetic flux Φ , and noted the analogy between the boundary condition and the one-dimensional Bloch problem discussed above. Let us first consider the impurity-free single-electron Hamiltonian in a magnetic field. The Schrödinger equation is then simply

$$\frac{\hat{p}^2}{2m^*}\psi(x) = \mathcal{E}\psi(x)$$

with usual periodic boundary conditions. The solutions are, of course, plane waves with wave vector $k = p/\hbar$, and due to periodic boundary conditions $k_n = 2\pi n/L$, where n is an integer. If we apply a magnetic field B perpendicular to the ring then $\hat{p} \rightarrow \hat{p} + e\mathbf{A}/c$ and the vector potential is

$$\mathbf{A} = \frac{1}{2}Br_0 = BL/4\pi$$

where r_0 is the ring radius. Magnetic flux Φ through the ring is then $\Phi = BL^2/4\pi$. The wave vector is then modified accordingly

$$k_n = \frac{2\pi}{L}n + \frac{e}{\hbar}\mathbf{A} = \frac{2\pi}{L}\left(n + \frac{e}{\hbar c}\frac{BL^2}{8\pi^2}\right) = \frac{2\pi}{L}\left(n + \frac{\Phi}{\Phi_0}\right).$$

The energy levels are then readily obtained from

$$\mathcal{E}_n(B) = \frac{\hbar^2 k_n^2}{2m^*} = \frac{\hbar^2}{2m^*r_0^2}\left(n + \frac{\Phi}{\Phi_0}\right)^2. \quad (2)$$

that are parabolas as a function of Φ . The equilibrium current (which is not a transport current) carried by the n -th level is then (Eq. 1)

$$I_n = -\frac{2\pi e\hbar}{m^*L^2}\left(n + \frac{\Phi}{\Phi_0}\right). \quad (3)$$

The total persistent current is $I = \sum_n I_n$, where the summation is over N lowest occupied levels². For *weak* impurity potentials, the degeneracies at the level crossings are lifted (Fig. 1). The magnetic moment for each occupied level is

$$\mathcal{M} = -\frac{d\mathcal{E}}{dB} = -\frac{e\hbar}{2m^*}\left(n + \frac{\Phi}{\Phi_0}\right). \quad (4)$$

² We consider the case of $T = 0$ and unless otherwise specified, only spinless particles.

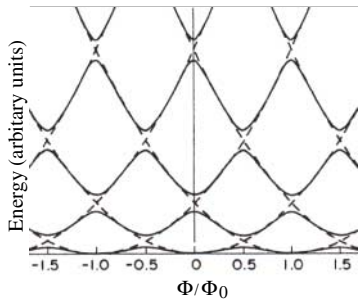


Fig. 1. Energy levels of a one-dimensional electron gas (non-interacting) on a ring as a function of the magnetic flux. The dashed lines correspond to the disorder-free case and the solid lines are for the weak impurity case

As we see from Fig. 1, because of the alternating signs of $\partial\mathcal{E}/\partial\Phi$ for each consecutive levels, the total moment is of the order of last moment around \mathcal{E}_F . The total persistent current is therefore,

$$I(\Phi) = -I_0 \begin{cases} 2\Phi/\Phi_0 & \text{for } N \text{ odd and } -\frac{1}{2} \leq \Phi/\Phi_0 < \frac{1}{2} \\ [2\Phi/\Phi_0 - 1] & \text{for } N \text{ even and } 0 \leq \Phi/\Phi_0 < 1 \end{cases}, \quad (5)$$

where $I_0 = ev_F/L$ and $v_F = \pi\hbar N/m^*L$ is the Fermi velocity. It is periodic in Φ/Φ_0 with period 1.

Early experiments were carried out on relatively large (μm -size) metallic rings containing a large number of electrons and impurities [6]. The observed results have not yet been explained to everyone's satisfaction [7]. A semiconductor ring in a GaAlAs/GaAs heterojunction [8] (also of μm size but in the *ballistic* regime) displayed the persistent current to be periodic with a period of Φ_0 and the amplitude of $0.8 \pm 0.4ev_F/L$, in agreement with the theoretical predictions. The electron-electron interaction did not change the value of persistent current. These experiments inspired a large number of researchers to report a large number of theoretical studies involving various averaging procedures, dependence on the chemical potential, temperature, different realizations of disorder, and often conflicting conclusions about the role of electron-electron interactions. We will not go into those aspects of the work on a mesoscopic ring any further.

2 Electronic Structure of a Parabolic Quantum Ring

In an attempt to clearly understand the role of electron-electron interactions in a quantum ring (QR) without getting encumbered by a variety of other issues mentioned above, we have constructed a model of a QR [9] that is disorder free, contains only a few interacting electrons and most importantly can be solved via the exact diagonalization method to obtain the energy levels very accurately. One advantage of this model is that, with the energy levels thus calculated, other physical quantities in addition to the persistent current, such as optical absorption, role of electron spin etc. can also be studied very accurately [10,11]. Interestingly, over the years, the model has received a

large following. The model is also most relevant for recent experiments on nano-rings [12,13,14,15,16,17,18,19].

2.1 Theoretical Model

The Hamiltonian for an electron in a ring with parabolic confinement and subjected to a perpendicular magnetic field is

$$\mathcal{H} = \frac{1}{2m^*} \left(\mathbf{p} - \frac{e}{c} \mathbf{A} \right)^2 + \frac{1}{2} m^* \omega_0^2 (r - r_0)^2 \quad (6)$$

where the vector potential is $\mathbf{A} = \frac{1}{2}(-By, Bx, 0)$ (symmetric gauge). The Schrödinger equation (in polar coordinates) is then written as

$$\begin{aligned} & -\frac{\hbar^2}{2m^*} \left\{ \frac{\partial^2 \Psi}{\partial r^2} + \frac{1}{r} \frac{\partial \Psi}{\partial r} + \frac{1}{r^2} \frac{\partial^2 \Psi}{\partial \theta^2} \right\} - \frac{ieB\hbar}{2m^*c} \frac{\partial \Psi}{\partial \theta} \\ & + \left[\frac{e^2 B^2 r^2}{8m^*c^2} + \frac{1}{2} m^* \omega_0^2 (r - r_0)^2 - E \right] \Psi = 0. \end{aligned} \quad (7)$$

Introducing the ansatz

$$\Psi = \frac{1}{\sqrt{2\pi}} f(r) e^{-il\theta},$$

and the quantities, $\mathcal{N} = BeA/hc = \Phi/\Phi_0$, $\alpha = \omega_0 m^* \mathcal{A}/h$, $x = r/r_0$, $\mathcal{E} = 2m^* \pi A E/h^2$, where $\mathcal{A} = \pi r_0^2$ is the area of the ring, the radial part of the Schrödinger equation is

$$f'' + \frac{1}{x} f' + \left[4\mathcal{E} + 2\mathcal{N} - 4\alpha^2 - (\mathcal{N}^2 + 4\alpha^2) x^2 + 8\alpha^2 x - \frac{l^2}{x^2} \right] f = 0, \quad (8)$$

where l is the usual orbital angular momentum of the single-particle level.

Parameter α is inversely proportional to the width of the ring. As shown in Fig. 2, large α means a narrow path for the electrons to traverse and

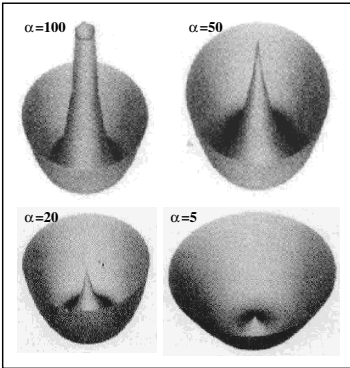


Fig. 2. Confinement potential $\alpha (r - r_0)^2$ for various values of α

hence the electron motion is close to that of a strictly one-dimensional ring. For small α , the electron motion is almost two-dimensional. These two limits can indeed be achieved in our model [9].

For a δ -function confinement ($x = 1$), the radial equation (Eq. 8) becomes

$$[4\mathcal{E} + 2\mathcal{N}l - 4\alpha^2 - (\mathcal{N}^2 + 4\alpha^2) + 8\alpha^2 - l^2] f = 0 \quad (9)$$

with the solution, $\mathcal{E} = \frac{1}{4}(l - \mathcal{N})^2$, derived above for a strictly one-dimensional ring (Eq. 2). In the other limit, i.e., when the magnetic field is large compared to the confinement α , the radial equation reduces to

$$f'' + \frac{1}{x}f' + \left[4\mathcal{E} + 2\mathcal{N}l - \mathcal{N}^2x^2 - \frac{l^2}{x^2}\right] f = 0$$

with the solution [9], $\mathcal{E} = (n + \frac{1}{2})\mathcal{N}$, corresponding to the Fock-Darwin levels [20]. The single-electron energy levels are obtained from numerical solutions of the radial equation (Eq. 8) and are shown in Fig. 3. For $\alpha = 20$ (Fig. 3(b)), the lower set of energy levels are still similar to those of the ideally narrow ring and are given by a set of translated parabolas (as in Fig. 3(a)). As α decreases, i.e., the ring becomes wider, the *sawtooth* behavior of the narrow ring is gradually replaced by the formation of Fock-Darwin levels as in the quantum dots.

In a quantum ring, or in any cylindrically symmetric system, the wave functions are of the form

$$\psi_\lambda = R_{nl}(r) e^{il\theta}, \quad n = 0, 1, 2, \dots, \quad l = 0, \pm 1, \pm 2, \dots, \quad (10)$$

and the interaction matrix elements are evaluated from [9]

$$\begin{aligned} \mathcal{V}_{\lambda_1 \lambda_2 \lambda_3 \lambda_4} &= \delta_{l_1+l_2, l_3+l_4} 2\pi \int_0^\infty dq q \mathcal{V}(q) \\ &\times \int_0^\infty dr_1 r_1 J_{|l_1-l_4|}(qr_1) R_{n_1 l_1}(r_1) R_{n_4 l_4}(r_1) \\ &\times \int_0^\infty dr_2 r_2 J_{|l_2-l_3|}(qr_2) R_{n_2 l_2}(r_2) R_{n_3 l_3}(r_2) \end{aligned} \quad (11)$$

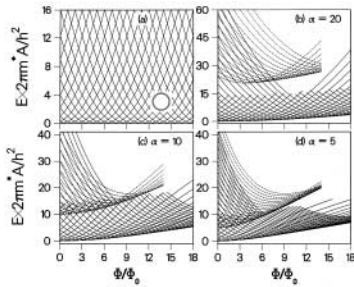


Fig. 3. Energy levels of a single electron versus the magnetic field for (a) ideally narrow ring, and (b)–(d) parabolic confinement model with various values of the confinement potential strength. The second Fock-Darwin level is plotted as *dotted lines*

where λ represents the quantum number pair $\{n, l\}$, J_i is the Bessel function of order i . All our numerical results correspond to the case of Coulomb interaction in a plane, $\mathcal{V}(q) = 2\pi\kappa/q$, where $\kappa = e^2/4\pi\epsilon_0\epsilon$. We have considered the case of $m^* = 0.07m$, $\epsilon = 13$, and the ring radius, $r_0 = 10$ nm.

Energies of a QR containing four interacting and non-interacting electrons [9] are shown in Fig. 4. It is clear that for the spinless electrons, the only effect of the inter-relectron interaction is an upward shift of the total energy. This is due to the fact that in a narrow ring all the close-lying states are in the lowest Landau band and cannot be coupled by the interaction because of the conservation of the angular momentum. The situation is however different once the spin degree of freedom is included, as described in Sect. 3.

2.2 Persistent Current

The magnetic moment (proportional to the persistent current) (Eq. 4) is calculated in our model from its thermodynamic expression

$$\mathcal{M} = - \sum_m \frac{\partial E_m}{\partial B} e^{-E_m/kT} / \sum_m e^{-E_m/kT}, \quad (12)$$

where $\partial E_m/\partial B$ are evaluated as the expectation values of the magnetization operator in the interacting states $|m\rangle$. In our ring geometry, the magnetization operator is $M = 1/2m^* [e/cL_z + (e^2Br^2)/2c^2]$. Our calculations revealed that the interaction has no effect on magnetization which remains periodic with period Φ_0 [9].

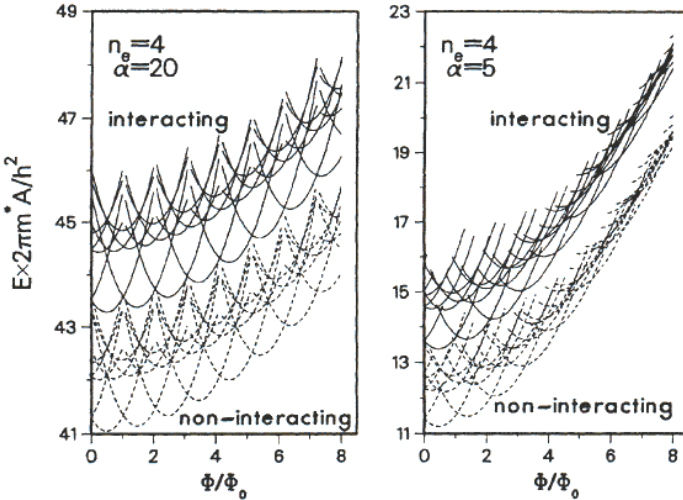


Fig. 4. Energy spectrum of a QR containing four non-interacting and interacting spinless electrons and for two different widths of the ring

We also studied the persistent current of a QR in the presence of a Gaussian impurity and/or with Coulomb interaction included [21]. The impurity interaction of our choice was,

$$\mathcal{V}^{\text{imp}}(r) = \mathcal{V}_0 e^{-(\mathbf{r}-\mathbf{R})^2/d^2}, \quad (13)$$

where \mathcal{V}_0 is the potential strength and d is the width. The impurity matrix element in our model is then

$$T_{\lambda,\lambda'} = 2\pi\mathcal{V}_0 e^{im\theta_0} \int R_\lambda(r) R_{\lambda'}(r) e^{-(R^2+r^2)/d^2} I_m \left(\frac{2rR}{d^2} \right) r dr, \quad (14)$$

where $m = l' - l$, (R, θ_0) is the impurity position and I_m is the modified Bessel function. We found that the effect of impurity is simply to lift the degeneracies in the energy spectrum and reduce the persistent current (Fig. 5), but it does not change the phase of the oscillations as a function of the magnetic flux. Even for the strongest impurity, the inter-electron interaction had no effect on the persistent current (except to shift the spectrum to higher energies).

Our result verified the conjecture of Leggett [22]. Based on variational arguments and two important properties of the many-particle wave function in a mesoscopic ring, viz., the antisymmetry and the single valuedness, he proposed that, for arbitrary electron-electron interactions and an arbitrary external potential, the maxima and minima of the energy curves for even and odd numbers of electrons would be the same as for non-interacting systems.

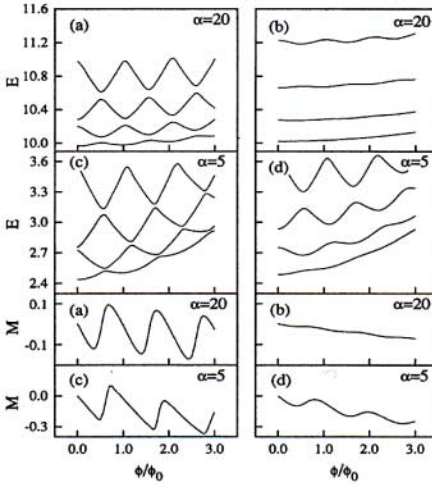


Fig. 5. Single-electron energy spectrum and magnetization (unit of energy is $2\hbar^2/m^*r_0^2$) versus Φ/Φ_0 for (a) $\alpha = 20, V_0 = 1, d = 0.2$; (b) $\alpha = 20, V_0 = 4, d = 0.5$; (c) $\alpha = 5, V_0 = 0.5, d = 0.2$; and (d) $\alpha = 5, V_0 = 1, d = 0.5$ [21]

3 Optical Absorption Spectra

After watching a not so spectacular performance of the persistent current, and from our past experience on the important effect of the inter-electron interaction on a few-electron quantum dot [20], we chose to turn our attention on optical spectroscopy of QRs [10], well before any such experiments on nano-rings were reported. We found that optical spectroscopy is indeed a direct route to explore impurity and interaction effects on a quantum ring. In our work, intensities of the optical absorption are evaluated within the electric-dipole approximation. For parabolic quantum dots (obtained by setting $r_0 = 0$ in Eq. 6), the radial part of the wave function (Eq. 10) is given explicitly as $R_{nl} = \mathcal{C} \exp[-r^2/(2a^2)] r^{|l|} L_n^{|l|}(r^2/a^2)$, where \mathcal{C} is the normalization constant, $a = \sqrt{\hbar/(m^*\Omega)}$, $\Omega = \sqrt{\omega_0^2 + \omega_c^2}/4$, $L_n^k(x)$ is the associated Laguerre polynomial, and ω_c is the cyclotron frequency. In our QR model ($r_0 \neq 0$) the radial part R_{nl} has to be determined numerically. We define the single-particle matrix elements as

$$d_{\lambda,\lambda'} = \langle \lambda' | r e^{i\theta} | \lambda \rangle = 2\pi \delta_{l+1,l'} \int_0^\infty r^2 R_{\lambda'}(r) R_\lambda(r) dr.$$

The dipole operators are then

$$\begin{cases} X = \frac{1}{2} \sum_{\lambda\lambda'} [d_{\lambda'\lambda} + d_{\lambda\lambda'}] a_{\lambda'}^\dagger a_\lambda, \\ Y = \frac{1}{2i} \sum_{\lambda\lambda'} [d_{\lambda'\lambda} - d_{\lambda\lambda'}] a_{\lambda'}^\dagger a_\lambda. \end{cases} \quad (15)$$

The probability of absorption from the ground state $|0\rangle$ to an excited state $|f\rangle$ will then be proportional to

$$\mathcal{I} = |\langle f | \mathbf{r} | 0 \rangle|^2 = |\langle f | X | 0 \rangle|^2 + |\langle f | Y | 0 \rangle|^2.$$

In the calculated absorption spectra presented below, the areas of the filled circles are proportional to \mathcal{I} .

3.1 Quantum Dots with a Repulsive Scattering Center

Far-infrared (FIR) spectroscopy on μm -size QR arrays that were created in GaAs/AlGaAs heterojunctions was first reported by Dahl et al. [23]. The rings were of two different sizes: The outer diameter being $\approx 50 \mu\text{m}$ diameter in both the cases, but the inner diameters were $12 \mu\text{m}$ (“broad rings”) and $30 \mu\text{m}$ (“narrow rings”). These rings were also described by these authors as disks with a repulsive scatterer at the center of the disk. The observed resonance frequencies as a function of the applied magnetic field are shown in Fig. 6. Around zero magnetic field the resonances are similar to what one expects for a circular disk. At larger B two modes with negative magnetic field dispersion were found that were interpreted as edge magnetoplasmons at the inner and outer boundary.

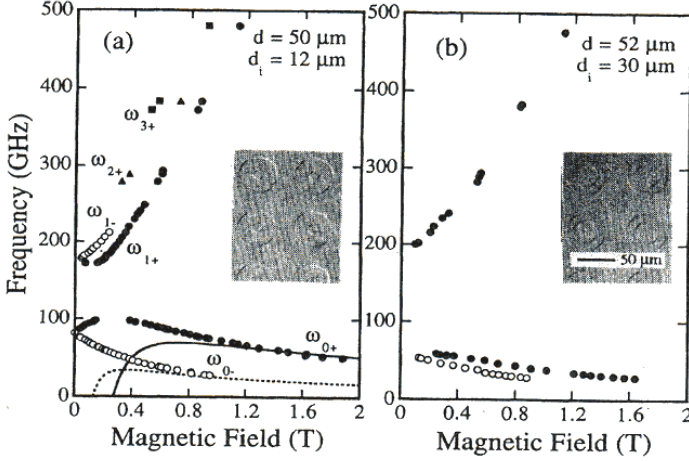


Fig. 6. Frequencies of magnetoplasma resonances for an array of (a) “broad” and (b) “narrow” rings [23]

Our theoretical results for absorption energies and intensities [10] of a quantum dot containing an impurity (modelled by a Gaussian potential) and one to three electrons are shown in Fig. 7 as a function of the magnetic field. We have included spin but ignored the Zeeman energy. The two upper modes of the one-electron spectrum behave almost similar to the experimental results of Dahl et al. [23]. However, the two lower modes behave differently (in the one-electron case) from those experimental results. The lower modes, i.e., the edge magnetoplasmon modes, reveal a periodic structure similar to the

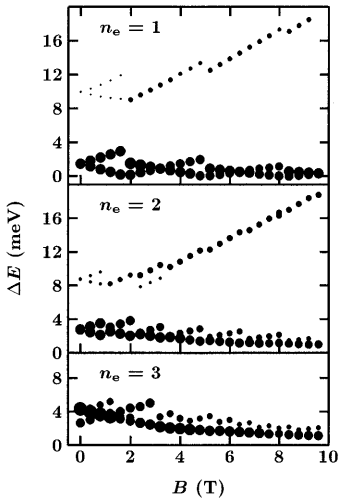


Fig. 7. Absorption energies and intensities of a quantum dot ($r_0 = 0$), $\hbar\omega_0 = 4$ meV, including a Gaussian repulsive scatterer (Eq. 13) with $\mathcal{V}_0 = 32$ meV, $d = 5$ nm, as a function of the applied magnetic field. The dot contains one to three electrons. The areas of the filled circles are proportional to the calculated intensity [10]

case of a parabolic ring discussed below. That is true only for the one-electron system.

When the number of electrons in the system is increased the periodic structure of the edge modes (the two lowest modes) starts to disappear due to the electron-electron interaction. Since the spin degree of freedom is also included in our calculations, the difference between the one- and two-electron results in Fig. 7 is entirely due to the Coulomb force. The lowest mode (which is also the strongest) behaves (even for only three electrons) much the same way as does the lowest mode in the experiment (where the system consists of the order of one million electrons).

3.2 A Parabolic Quantum Ring

The results reported below correspond to that of a narrow parabolic ring with $\alpha = 20$ and $r_0 = 10$ nm. In a pure one-electron ring the dipole-allowed absorption from the ground state can happen with equal probability to the first two excited states and all other transitions are forbidden. An impurity in the ring will mix the angular-momentum eigenstates of the pure system into new states between which dipole transitions are allowed. For an impurity of moderate strength (Fig. 8(a)), an appreciable part of the transition probability still goes to the first two excited states while for a strong impurity, absorptions taking the electron to the lowest excited state are more favorable (Fig. 8(b)). One important result here is that in a system with broken rotational symmetry, *transition probability depends strongly on the polarization of the incident light*. For example, if instead of the unpolarized light considered here, we were to consider the case of light polarized along the diameter passing through the impurity [24], the absorption would prefer the *second* excited state. The other interesting feature observed in Fig. 8 is the periodic

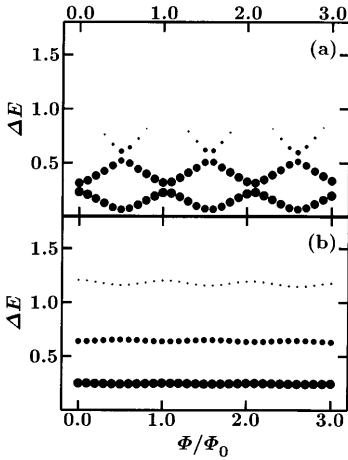


Fig. 8. Absorption energies of a single electron in a parabolic QR versus Φ/Φ_0 for $\alpha = 20$ and (a) $\mathcal{V}_0 = 1.0$, $d = 0.2$ and (b) $\mathcal{V}_0 = 4.0$, $d = 0.5$ [10]

behavior of absorption energies as a function of the applied field that follows closely the behavior of the persistent current. Blocking of this current by a strong impurity is reflected as the flat curves of absorption energies versus the field.

In order to study the effect of impurity potential and electron correlations, we have considered a ring with four spinless electrons. Compared to the case of impurity-free single-electron results, here the dipole transitions to the first excited state are forbidden ($|\Delta L| > 1$). However, impurities will again permit transitions to the forbidden states. In general, effect of an impurity on the absorption spectrum as a function of the external magnetic field can be qualitatively explained by the single-particle properties. For example, when we compare Figs. 9(a) and (b) we notice that lifting of the degeneracy in the energy spectra of non-interacting electrons is reflected by a smoother behavior as a function of the applied field. The sole effect of the Coulomb interaction on the energy spectrum is to shift it upwards and to increase the gap between the ground state and excited states (see Sect. 1). As a result, the Coulomb interaction moves the absorption to higher frequencies (Fig. 9 (c) and (d)). The effect of electron-electron interaction is evident in the intensity: for the non-interacting system (Fig. 9 (a) and (b)), intensity of each absorption mode does not depend on the magnetic field, but for the interacting system (Fig. 9 (c) and (d)) there is a strong variation of intensity as a function of the field.

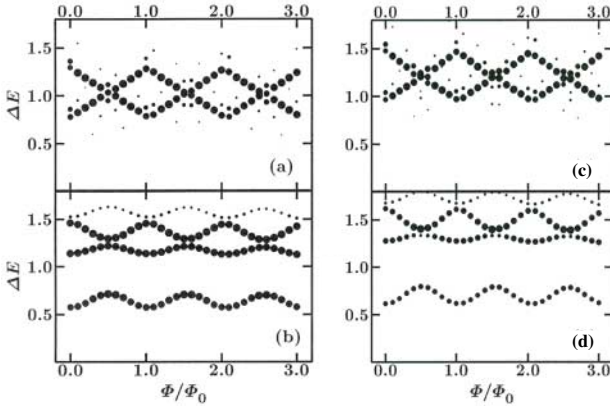


Fig. 9. Dipole-allowed absorption energies for four non-interacting [(a) and (b)] and interacting [(c) and (d)] electrons in a QR versus Φ/Φ_0 . The parameters are the same as in Fig. 8

4 Role of Electron Spin

Until now, we have considered only spinless particles in our theoretical model of a parabolic QR. However, at low fields, electron spins are expected to play

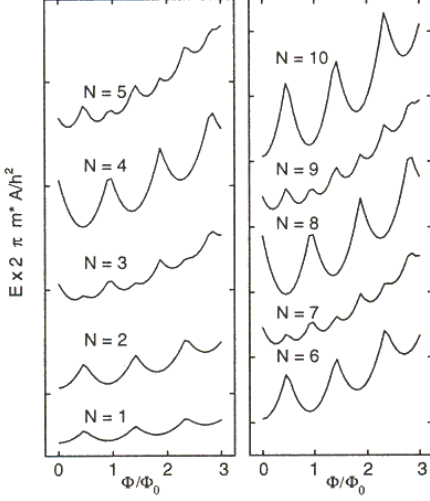


Fig. 10. Ground state energy versus Φ/Φ_0 for up to ten non-interacting electrons. The energies are scaled to illustrate how the periodicity depends upon the number of electrons on the ring [11]

an important role. In Fig. 10, we show the ground state energies calculated for up to ten non-interacting electrons on a ring [11]. Clearly, the major consequence of the spin degree of freedom is period and amplitude halving of the energy with increasing number of the flux quanta. It is also strongly particle number dependent. This result for a non-interacting system was reported earlier [25] and can be accounted for by simply counting the number of spins, following the Pauli principle, and noting that the up and down spins contribute identically to the energy. The particle number (*modulo* 4) dependence can also be trivially explained in this way.

The Coulomb interaction in our model was found to have a profound effect on the energy spectra when the spin degree of freedom is included [11]. The calculated low-lying energy states for a two non-interacting (a) and interacting (b) electron system are shown in Fig. 11. As the flux is increased, the angular momentum quantum number (L) of the ground state of a non-interacting system is increased by two, i.e., the ground state changes as 0,2,4,... The period is as usual, one flux quantum. The ground state of the non-interacting system is always a spin-singlet. The first excited state is spin degenerate. As the Coulomb interaction is turned on, the singlet-triplet degeneracy is lifted. This is due to the fact that, as the interaction is turned on, states with highest possible symmetry in the spin part of the wave function are favored because that way one gains the exchange energy. As a result, the triplet state comes down in energy with respect to others and therefore the period (as well as the amplitude) of the ground state oscillations is halved. Similar results are also evident with three electrons ($S_z = \frac{1}{2}$) (Fig. 11(c) non-interacting and (d) interacting electron systems), where the ground state oscillates with a period $\Phi_0/3$. We found similar behavior for QRs containing up to four electrons [11]. In the four electron system, we noticed that with-

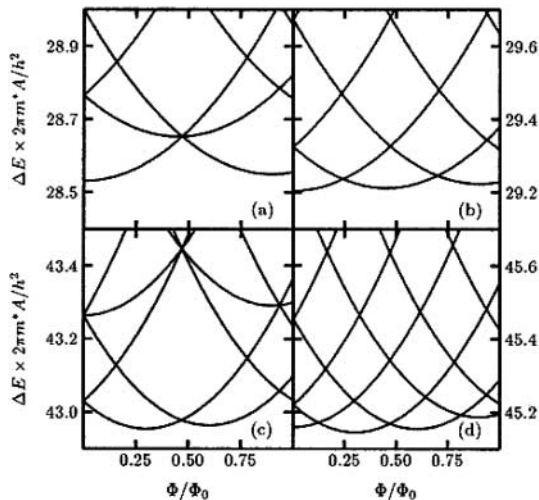


Fig. 11. Few low-lying energy states for a ring containing two (a) non-interacting and (b) interacting electrons. Three electron results are given in (c) and (d) for non-interacting and interacting systems respectively

out the Zeeman energy included the spin configuration $S_z = 0$ has the lowest energy and a $\Phi_0/2$ periodicity is observed. However, if the Zeeman energy is taken into account the $S_z = 1$ configuration becomes lower in energy and the $\Phi_0/4$ periodicity is recovered.

The final message that emerges from these studies is that: the Coulomb interaction (in fact, any type of repulsive interaction) favors the spin-triplet ground states for reasons explained above. In the absence of any interaction, the ground states are spin singlets and as a function of Φ/Φ_0 are parabolas with minimum at about the integer values (exactly at integer values for an ideal ring). When a repulsive interaction is turned on, singlet states rise in energy more than the triplet state and for strong enough repulsion, a decrease in period of oscillations is observed.

Can one observe the fractional oscillations of the ground state energy in optical spectroscopy? We present in Fig. 12 our theoretical results for the optical absorption in a QR containing two electrons and also an impurity of moderate strength [10] ($V_0^i = 1.0, d_i = 0.2$). The strong effect of the Coulomb interaction on the electrons with spin is quite obvious. The system of non-interacting electrons but a impurity-free system ($S_z = 0$) is shown in (a), while the interacting (impurity-free) case is shown in (b). A system containing an impurity of moderate strength is shown for the non-interacting (c) and interacting (d) electrons. The absorption spectra clearly reflect the behavior of the energy levels and the impurity does not destroy the fractional periodicity of the electronic states.

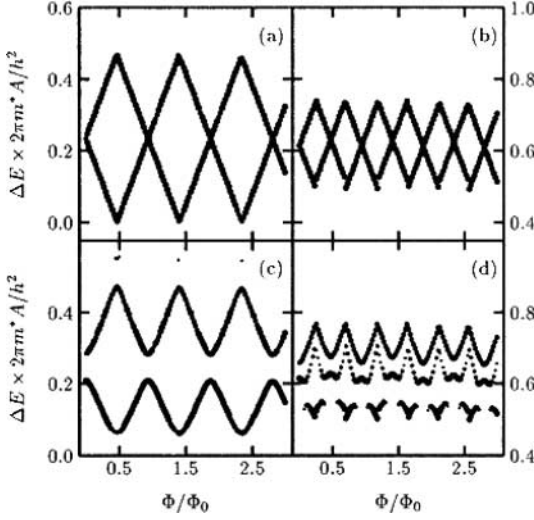


Fig. 12. Absorption spectra of a QR containing two (a), (c) non-interacting, or (b), (d) interacting electron. In (c), (d), additionally, the system also has an impurity of moderate strength. The size of the filled circles is proportional to the calculated absorption intensities

5 Recent Works on Nano-Rings

Quantum rings of nanoscopic dimensions are usually created as self-organized [12,13,14,15] or fabricated on AlGaAs/GaAs heterojunctions containing a two-dimensional electron gas [16,17,18]. Self-organized QRs in InAs/GaAs systems were created by growing InAs quantum dots on GaAs and a process involving a growth interruption when In migrates at the edge of the dot. This creates nanostructures that resemble a volcano crater with the center hole of 20 nm diameter and the outer diameter of 60-120 nm [12]. Only one or two electrons are admitted in these clean nano rings and FIR spectroscopy was performed to investigate the ground state and low-lying excitations in a magnetic field that is oriented perpendicular to the plane of the rings. The low-lying excitations were found to be unique to QRs first explored theoretically by us [9,10,11]. Similarly, the observed ground state transition from angular momentum $l = 0$ to $l = -1$, when one flux quantum threads the ring, is also well described by our parabolic ring model. Warburton et al. [13] reported a successive population of these self-assembled structures by up to five electrons. They investigated the exciton luminescence of charged rings. Recombination-induced emission by the systems from a neutral exciton to a quintuply charged exciton was reported. In magnetotransport experiments in Coulomb blockade regime reported in Refs. [16,17], QRs contain a few hundred electrons. The deduced energy spectra was however well described by the single-electron picture. Keyser et al. [18] recently reported transport spectroscopy on a small ring containing less than ten electrons. The deduced energy spectrum was found to be strongly influenced by the electron-electron interaction. They also observed a reduction of the AB period that is in line with our theoretical results of Sect. 3.

Following our original work on parabolic quantum rings, many theoretical works on such systems have been reported [26,27,28,29,30,31]. Chaplik [26] investigated a parabolic QR having a small finite width. He noted that the magnetic field dependent component of the energy does not depend on the inter-electron interaction. He also investigated the behavior of charged and neutral magnetic excitons in a QR. In Ref. [28], a single QR containing up to eight electrons was investigated using path integral Monte Carlo techniques. Addition energies, spin correlations, etc. were evaluated for different values of ring radii, particle number and the temperature. There are many other issues related to the QR that were investigated theoretically in recent years. With the advent of nanoscopic quantum rings research on parabolic QRs has taken a new dimension. Like all other nanostructures investigated in recent years, QRs have proven to be a very useful device to investigate many fundamental physical phenomena and perhaps in a near future will also be found to be important for practical applications.

Acknowledgements

Many thanks to Rolf Haug (Hannover) for inviting me to present the talk. I also thank Christian Schüller and Detlef Heitmann for their hospitality during a visit at the University of Hamburg as a guest Professor in March 2003.

References

1. F. Hund, Ann. Phys. (Leipzig) **32**, 102 (1938). 79
2. M. Büttiker, Y. Imry, R. Landauer, Phys. Lett. **A96**, 365 (1985). 79, 80
3. N. Byers, C.N. Yang, Phys. Rev. Lett. **7**, 46 (1961). 79
4. F. Bloch, Phys. Rev. **21**, 1241 (1968). 79
5. R.B. Laughlin, Phys. Rev. B **23**, 5632 (1981); B.I. Halperin, Phys. Rev. B **25**, 2185 (1982); for a review, see T. Chakraborty, P. Pietiläinen: *The Quantum Hall Effects* (Springer, N.Y. 1995), second edition. 80
6. L.P. Levy et al., Phys. Rev. Lett. **64**, 2074 (1990); V. Chandrasekhar, et al., Phys. Rev. Lett. **67**, 3578 (1991). 81
7. U. Eckern, P. Schwab, Adv. Phys. **44**, 387 (1995); H.F. Cheung, et al., Phys. Rev. B **37**, 6050 (1988); G. Montambaux, H. Bouchiat, et al., Phys. Rev. B **42**, 7647 (1990). 81
8. D. Mailly, C. Chapelier, A. Benoit, Phys. Rev. Lett. **70**, 2020 (1993). 81
9. T. Chakraborty, P. Pietiläinen, Phys. Rev. B **50**, 8460 (1994); and also in *Transport Phenomena in Mesoscopic Systems*. Eds. H. Fukuyama and T. Ando (Springer, Heidelberg, 1992). 81, 83, 84, 92
10. V. Halonen, P. Pietiläinen, T. Chakraborty, Europhys. Lett. **33**, 377 (1996). 81, 86, 87, 88, 91, 92
11. K. Niemelä, P. Pietiläinen, P. Hyvönen, T. Chakraborty, Europhys. Lett. **36**, 533 (1996). 81, 90, 92
12. A. Lorke, et al., Phys. Rev. Lett. **84**, 2223 (2000). 82, 92

13. R.J. Warburton, et al., *Nature* **405**, 926 (2000). 82, 92
14. H. Pettersson, et al., *Physica E* **6**, 510 (2000). 82, 92
15. D. Haft, et al., *Physica E* **13**, 165 (2002). 82, 92
16. A. Fuhrer, et al., *Nature* **413**, 822 (2001). 82, 92
17. T. Ihn, et al., *Physica E* (2003). 82, 92
18. U.F. Keyser, et al., *Phys. Rev. Lett.* (2003). 82, 92
19. J. Liu, A. Zaslavsky, L.B. Freund, *Phys. Rev. Lett.* **89**, 096804 (2002). 82
20. P.A. Maksym, T. Chakraborty, *Phys. Rev. Lett.* **65**, 108 (1990);
T. Chakraborty, *Comments Condens. Matter Phys.* **16**, 35 (1992);
T. Chakraborty, *Quantum Dots* (North-Holland, Amsterdam, 1999);
T. Chakraborty, F. Peeters, U. Sivan (Eds.), *Nano-Physics & Bio-Electronics:
A New Odyssey* (Elsevier, Amsterdam, 2002); S.M. Reimann, M. Manninen:
Rev. Mod. Phys. **74**, 1283 (2002). 83, 86
21. T. Chakraborty, P. Pietiläinen, *Phys. Rev. B* **52**, 1932 (1995). 85
22. A.J. Leggett, in *Granular Nanoelectronics*, vol. 251 of *NATO Advanced Study
Institute, Series B: Physics*, edited by D.K. Ferry, J.R. Berker, and C. Jacoboni
(Plenum, New York, 1992), p. 297. 85
23. C. Dahl, J.P. Kotthaus, H. Nickel, W. Schlapp, *Phys. Rev. B* **48**, 15480 (1993).
86, 87
24. P. Pietiläinen, V. Halonen, T. Chakraborty, in *Proc. of the International Work-
shop on Novel Physics in Low-Dimensional Electron Systems*, T. Chakraborty
(Ed.), *Physica B* **212** (1995). 88
25. D. Loss, P. Goldbart, *Phys. Rev. B* **43**, 13762 (1991). 90
26. A.V. Chaplik, *JETP* **92**, 169 (2001). 93
27. S. Viefers, et al., *Phys. Rev. B* **62**, 10668 (2000). 93
28. P. Borrmann, J. Harting, *Phys. Rev. Lett.* **80**, 3120 (2001). 93
29. A. Puente, L. Serra, *Phys. Rev. B* **63**, 125334 (2001). 93
30. Z. Barticevic, M. Pacheco, A. Latge, *Phys. Rev. B* **62**, 6963 (2000); Z. Bartice-
vic, G. Fuster, M. Pacheco, *Phys. Rev. B* **65**, 193307 (2002). 93
31. A. Emperador, M. Pi, M. Barranco, E. Lipparini, *Physica E* **12**, 787 (2002).
93